ORTHOGONAL RING PATTERNS

ALEXANDER I. BOBENKO, TIM HOFFMANN, AND THILO RÖRIG

Abstract. We introduce orthogonal ring patterns consisting of pairs of concentric circles generalizing circle patterns. We show that orthogonal ring patterns are governed by the same equation as circle patterns. For every ring pattern there exists a one parameter family of patterns that interpolates between a circle pattern and its dual. We construct ring pattern analogues of the Doyle spiral, Erf and z^α functions. We also derive a variational principle and compute ring patterns based on Dirichlet and Neumann boundary conditions.

1. Introduction

The theory of circle patterns can be seen as a discrete version of conformal maps. Schramm [6] has studied orthogonal circle patterns on the $\mathbb{Z}^2$-lattice, has proven their convergence to conformal maps and constructed discrete analogs of some entire holomorphic functions. Circle patterns are described by a variational principle [5], which is given in terms of volumes of ideal hyperbolic polyhedra [4]. We introduce orthogonal ring patterns that are natural generalizations of circle patterns. Our theory of orthogonal ring patterns has its origin in discrete differential geometry of S-isothermic cmc surfaces [3]. Recently, orthogonal double circle patterns (ring patterns) on the sphere have been used to construct discrete surfaces S-cmc by Tellier et al. [7].

We start Sect. 2 with a definition of orthogonal ring patterns and their elementary properties. In particular we show that all rings have the same area. Our main Theorem 2.4 shows that ring patterns are described by an equation for variables at the vertices. Furthermore, each ring pattern comes with a natural 1-parameter family of patterns. In Sect. 3 we show that as the area of the rings goes to zero the ring patterns converge to orthogonal circle patterns. In the following Sect. 4 we introduce ring patterns analogs of Doyle spirals, the Erf function, z^α for $\alpha \in (0, 2]$, and the logarithm. Finally, we describe a variational principle to construct ring patterns for given Dirichlet or Neumann boundary conditions. A remarkable fact that we explore is that the orthogonal ring and circle patterns in $\mathbb{R}^2$ are governed by the same integrable equation. In a subsequent publication we plan to develop a theory of ring patterns in a sphere and hyperbolic space. They are governed by generalizations of the corresponding equations for $\mathbb{R}^2$ given in elliptic functions. It is tempting to establish a connection to discrete integrable equations classified in [1].

Key words and phrases. discrete differential geometry, circle patterns, variational principles .

2. Orthogonal ring patterns

In this section, we will introduce orthogonal ring patterns and show that the existence of such the patterns is governed by the same equation as the existence of orthogonal circle patterns.

We will consider cell complex G defined by a subset of the quadrilaterals of the $\mathbb{Z}^2$ lattice in $\mathbb{R}^2$. The vertices of the complex G are indexed by $(m,n) \in \mathbb{Z}^2$ and denoted by $v_{m,n}$. The oriented edges are given by pairs of vertices and are either *horizontal* $(v_{m,n}, v_{m+1,n})$ or *vertical* $(v_{m,n}, v_{m,n+1})$.

A *ring* is a pair of two concentric circles in $\mathbb{R}^2$ that form a ring (annulus). We identify the vertices with the centers and denote the inner circle and its radius by small letters c and r, and the outer circle and its radius by capital letters C and R. We assign an orientation to the ring by allowing r to be negative: positive radius corresponds to counter-clockwise and negative radius to clockwise orientation. The outer radius will always be positive. The area of a ring is given by $(R^2 - r^2)\pi$. Subscripts are used to associate circles and radii to vertices of the complex, e.g., $c_{m,n}$ is the inner circle associated with the vertex $v_{m,n}$.

Definition 2.1 (Orthogonal ring patterns)**.** *Let G be a subcomplex of the $\mathbb{Z}^2$-lattice defined by its squares. An* orthogonal ring pattern *consists of rings associated to the vertices of G satisfying the following properties:*

1. *The rings associated to neighboring vertices v_i and v_j* intersect orthogonally*, i.e., the outer circle C_i of the one vertex intersects the inner circle c_j of the other vertex orthogonally and vice versa (see Fig. 1, left).*
2. *In each square of G the inner circles $c_{m,n}$ and $c_{m+1,n+1}$ and the outer circles $C_{m,n+1}$ and $C_{m+1,n}$ pass through one point. Then orthogonality implies that the two inner and the two outer circles touch in this point (see Fig. 1, center).*
3. *For two neighbors $v_{m+1,n}$ and $v_{m,n+1}$ of $v_{m,n}$ in one quadrilateral we assume that the points $c_{m,n} \cap C_{m+1,n} \setminus C_{m,n+1}$, $C_{m+1,n} \cap C_{m,n+1}$, and $c_{m,n} \cap C_{m,n+1} \setminus C_{m+1,n}$ have the same orientation as $c_{m,n}$, i.e., are in counter-clockwise order if $r_{m,n}$ is positive and in clockwise order if $r_{m,n}$ is negative. Similarly, for the neighbors $v_{m-1,n}$ and $v_{m,n+1}$ of $v_{m,n}$ with the roles of inner and outer circles interchanged.*

The orthogonal intersection of neighboring rings has the following implication for their areas.

Lemma 2.2. *Consider two rings with radii r_i, R_i and r_j, R_j that intersect orthogonally. Then the two rings have the same area.*

Proof. By Pythagoras' Theorem the square of the distance d between the circle centers is $R_i^2 + r_j^2 = d^2 = r_i^2 + R_j^2$ since the inner and outer circles are intersecting orthogonally. This equation is equivalent to the equality of the ring areas $(R_i^2 - r_i^2)\pi = (R_j^2 - r_j^2)\pi$. □

The constant area allows us to use a single variable ρ_i to express the inner and the outer radii of the rings in the following way: Consider an orthogonal ring pattern with constant ring area $A_0 = \pi \ell_0^2$, that is, for the radii r_i, R_i

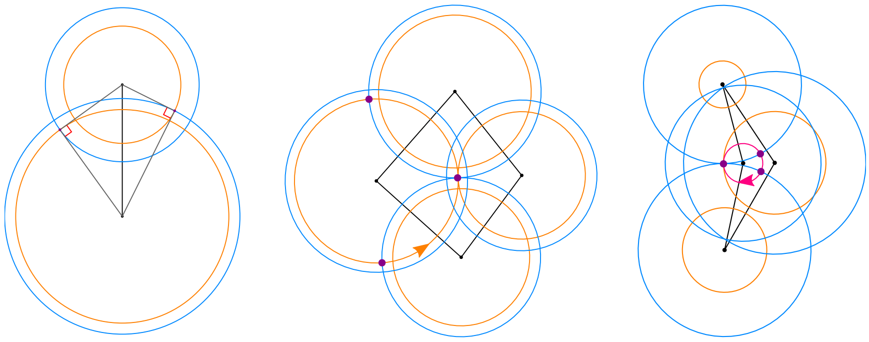

Figure 1. Left: Two orthogonally intersecting rings. Center: The inner circles touch along one diagonal of a quadrilateral and the outer circles along the other diagonal at the same touching point. Right: If the orientation (i.e., signed radii) of the inner circles differ, then the centers lie on the same side of the common tangent.

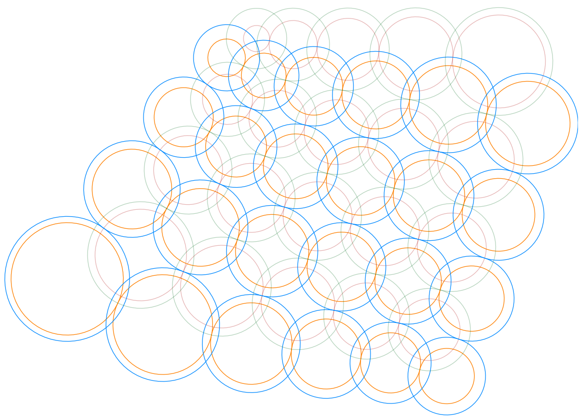

Figure 2. The rings of an orthogonal ring pattern partition into two diagonal families of touching rings.

of all vertices $v_i \in V$ we have $R_i^2 - r_i^2 = \ell_0^2$. Then for each vertex we can choose a single variable ρ_i by setting

$$R_i = \ell_0 \cosh(\rho_i) \quad \text{and} \quad r_i = \ell_0 \sinh(\rho_i)\,. \tag{1}$$

We will call those new variables *ρ-radii*. The orientation of the rings is encoded in the sign of the ρ-radii. In Sect. 3 we consider the limit of orthogonal ring patterns as the area goes to zero. The ρ-radii become the logarithmic radii of a Schramm type orthogonal circle pattern [6] in the limit.

As in the case of orthogonal circle patterns there exist sublattices $V_e = \{(m,n) \in \mathbb{Z}^2 \,|\, m+n \text{ even}\}$ and $V_o = \{(m,n) \in \mathbb{Z}^2 \,|\, m+n \text{ odd}\}$ such that all rings along the diagonals touch (see Fig. 2).

Neighboring vertices of an orthogonal ring pattern define a cyclic quadrilaterals of the following forms:

The circles C_i, c_i and C_j, c_j intersect in four points. Since the inner circle c_i (resp. c_j) and the outer circle C_j (resp. C_i) intersect orthogonally the centers of the circles and the intersection points $c_i \cap C_j$ and $C_i \cap c_j$) lie

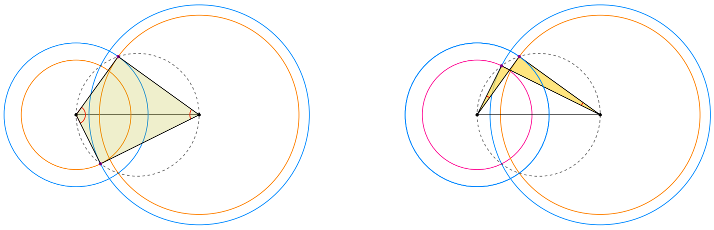

Figure 3. Cyclic quadrilaterals defined by two orthogonally intersecting circle rings depending on the signs of the radii: Embedded quadrilateral for $\rho_i, \rho_j > 0$ (left), non-embedded quadrilateral for $\rho_i < 0$, $\rho_j < 0$ (right).

on a circle (see Fig. 3 left). If $\rho_{m,n}$ is positive we obtain an embedded cyclic quadrilateral with positive orientation if $\rho_{m+1,n}$ is positive, i.e., we choose the intersection point $c_{m,n} \cap C_{m+1,n}$ above and the intersection point $C_{m,n} \cap c_{m+1,n}$ below the line connecting the centers. For both $\rho_{m,n} < 0$ and $\rho_{m+1,n} < 0$ we choose the opposite points. So for $\rho_{m,n}, \rho_{m+1,n} > 0$ we obtain a quadrilateral with positive orientation and for $\rho_{m,n}, \rho_{m+1,n} < 0$ with negative orientation. If $\rho_{m,n}$ and $\rho_{m+1,n}$ have opposite signs, then we obtain a non-embedded quadrilateral. The intersection points are chosen such that the angle at the vertex $v_{m,n}$ has the same sign as the corresponding $\rho_{m,n}$. If one of the ρ's is 0, the cyclic quadrilateral degenerates to a triangle with a double vertex.

Given the ρ-radii we can compute the angles in the cyclic quadrilaterals. We will assume that the arctan function maps to oriented angles in $(-\frac{\pi}{2}, \frac{\pi}{2})$.

Lemma 2.3. *Let v_i and v_j be two neighboring vertices in an orthogonal ring pattern with ρ-radii ρ_i and ρ_j. Then the angle at the vertex v_i in the cyclic quadrilateral defined by the two rings at v_i and v_j is given by*

$$\varphi_{ij} = \begin{cases} \pi - 2\arctan(e^{\rho_i - \rho_j}) & \text{if } \rho_i > 0 \\ -2\arctan(e^{\rho_i - \rho_j}) = -\varphi_{ji} & \text{if } \rho_i < 0 \end{cases}$$

Proof. We will compute the angles for $\rho_i > 0$ (the case $\rho_i < 0$ can be shown similarly.) For circles of radii R_i, r_i and R_j, r_j given by equation (1) the angle can be computed by

$$\varphi_{ij} = \arctan(\frac{r_j}{R_i}) + \arctan(\frac{R_j}{r_i}).$$

The sum of inverse tangents is given by

$$\arctan a + \arctan b = \begin{cases} \arctan \frac{a+b}{1-ab} & \text{if } ab < 1 \\ \frac{\pi}{2} & \text{if } ab = 1 \\ \pi - \arctan \frac{a+b}{1-ab} & \text{if } ab > 1, \text{ and } a+b \geq 0, \\ -\pi - \arctan \frac{a+b}{1-ab} & \text{if } ab > 1, \text{ and } a+b < 0. \end{cases}$$

In our case $ab = \frac{r_j}{R_i}\frac{R_j}{r_i} = \frac{\sinh(2\rho_j)}{\sinh(2\rho_i)}$. For $\rho_i > 0$ we have to consider two cases:

(1) $\rho_i > \rho_j \Leftrightarrow ab < 1$ and
(2) $\rho_i < \rho_j \Leftrightarrow ab > 1$.

In case (1) we can use the first case of above formula for the sum of two arctan's to obtain

$$\varphi_{ij} = \arctan(\frac{\frac{r_j}{R_i} + \frac{R_j}{r_i}}{1 - \frac{r_j}{R_i}\frac{R_j}{r_i}}) = \arctan(\frac{r_i r_j + R_i R_j}{r_i R_i - r_j R_j}).$$

In terms of the ρ-radii this yields

$$\begin{aligned}\varphi_{ij} &= \arctan(\frac{\sinh\rho_i \sinh\rho_j + \cosh\rho_i \cosh\rho_j}{\sinh\rho_i \cosh\rho_i - \sinh\rho_j \cosh\rho_j}) \\ &= \arctan(\frac{1}{\sinh(\rho_i - \rho_j)}).\end{aligned}$$

Note that we did not need to introduce the area constant for the ring pattern as it cancels in all quotients. Since we are currently considering (1) with $\rho_i > \rho_j$ we have $\sinh(\rho_i - \rho_j) > 0$ and:

$$\varphi_{ij} = \arctan(\frac{1}{\sinh(\rho_i - \rho_j)}) = \frac{\pi}{2} - \arctan(\sinh(\rho_i - \rho_j))$$

But $\arctan(\sinh x) = 2\arctan(e^x) - \frac{\pi}{2}$. Thus

$$\varphi_{ij} = \pi - 2\arctan(e^{\rho_i - \rho_j}).$$

This finishes the proof in case (1) for $\rho_i > 0$. Case (2) and the cases for $\rho_i < 0$ are handled analogously. □

With the above angles we are able to prove the following theorem on orthogonal ring patterns.

Theorem 2.4 (Orthogonal ring patterns)**.** *Let $\mathcal{R}$ be a ring pattern on a simply connected subcomplex G of $\mathbb{Z}^2$ defined by a subset of the squares of $\mathbb{Z}^2$. Then for interior vertices the ρ-radii of $\mathcal{R}$ satisfy*

$$2\pi = \sum_{j: v_j \bullet\!\!\bullet v_i} 2\arctan(e^{\rho_i - \rho_j}). \tag{2}$$

Conversely, given ρ-radii on the vertices of G satisfying the above equation, then there exists a unique orthogonal ring pattern.

Proof. Let v_i be an interior vertex of G with four neighboring vertices v_1, v_2, v_3, and v_4. The five rings form a flower in the pattern and hence the angles φ_{ij} for $j \in \{1, 2, 3, 4\}$ sum up to 2π (or -2π, depending on the orientation). We consider positive ρ_i first. By Lemma 2.3 the angles at vertex v_i in the cyclic quadrilateral defined by neighboring rings can be computed from the ρ-radii

$$\varphi_{ij} = \pi - 2\arctan(e^{\rho_i - \rho_j}).$$

So summing up around v_i we obtain

$$2\pi = \sum_{j=1}^{4} \varphi_{ij} = \sum_{j=1}^{4} \pi - 2\arctan(e^{\rho_i - \rho_j}).$$

This is equivalent to (2). For negative ρ_i we can simply use the other equation of Lemma 2.3 and show that identity (2) also holds.

For the converse, consider a single flower of a complex G with ρ-radii satisfying equation (2). Let v_i be an interior vertex with $\rho_i > 0$ (the case

$\rho_i < 0$ follows along the same lines). The four angles in the quadrilaterals at the edges (v_i, v_j) are given by Lemma 2.3:

$$\varphi_{ij} = \pi - 2\arctan(e^{\rho_i - \rho_j}) \quad \text{for } j = 1, 2, 3, 4.$$

Using equation (2) we see that $\sum_{j=1}^{4} \varphi_{ij} = 2\pi$. Hence we can assemble the four quadrilaterals and rings around the vertex v_i to form an orthogonal ring pattern. As the complex G is simply connected the local proof suffices to prove that the entire complex G can be assembled to build an orthogonal ring pattern.

The theorem also holds if $\rho_{m,n} = 0$ for some $(m, n) \in \mathbb{Z}^2$ by taking the appropriate limit. The angles φ_{ij} are not continuous, since the flower around v_i changes its orientation when ρ_i changes sign. But equation (2) stays valid and we obtain a ring pattern even if some ρ vanishes. □

The angle condition at the vertices of Thm. 2.4 only depends on the differences of the logarithmic radii. So without violating equation (2), we can apply a shift $\rho \to \rho^\delta = \rho + \delta$ by $\delta \in \mathbb{R}$ to the ρ-variables.

Corollary 2.5. *Consider an orthogonal ring pattern $\mathcal{R}$ of area π for given ρ-radii $\rho_{m,n}$. Then the ρ-radii $\rho^\delta_{m,n} = \rho_{m,n} + \delta$ define a one parameter family of orthogonal ring patterns $\mathcal{R}^\delta$ with radii:*

$$r_i^\delta = \sinh(\rho_i + \delta)$$
$$R_i^\delta = \cosh(\rho_i + \delta)$$

and area $A^\delta = \pi$.

3. Relation to orthogonal circle patterns

In this section we give a detailed description of the relation of orthogonal ring patterns and orthogonal circle patterns. It turns out that orthogonal circle patterns can be considered as a special case of ring patterns with constant ring area $A_0 = 0$.

To formulate the limit we need to review some properties of orthogonal circle patterns. Two orthogonally intersecting circles in an orthogonal circle pattern create a cyclic right angled kite (see Fig. 5 left and right). The angle φ°_{ij} at a vertex v_i in a kite on the edge (v_i, v_j) of an orthogonal circle pattern with radii $r^\circ_i = e^\rho_i$ is given by:

$$\begin{aligned} \varphi^\circ_{ij} &= 2\arctan(\frac{r^\circ_j}{r^\circ_i}) = 2\arctan(e^{\rho_j - \rho_i}) \\ &= \pi - 2\arctan(e^{\rho_i - \rho_j}) \end{aligned} \tag{3}$$

In case of circle patterns the ρ-radii are called *logarithmic radii*. Logarithmic radii of an immersed orthogonal circle pattern are governed by the same equation (cf. [6, 5]) as the ρ-radii of ring patterns (see Thm. 2.4).

Furthermore, for each orthogonal circle pattern $\mathcal{C}$ with logarithmic radii ρ_i there exists a dual pattern $\mathcal{C}^*$ with radii $e^{-\rho_i}$. The angles of the dual pattern are given by

$$(\varphi^\circ_{ij})^* = 2\arctan(\frac{r^*_j}{r^*_i}) = 2\arctan(e^{-\rho_j + \rho_i}) = \pi - \varphi^\circ_{ij}\,.$$

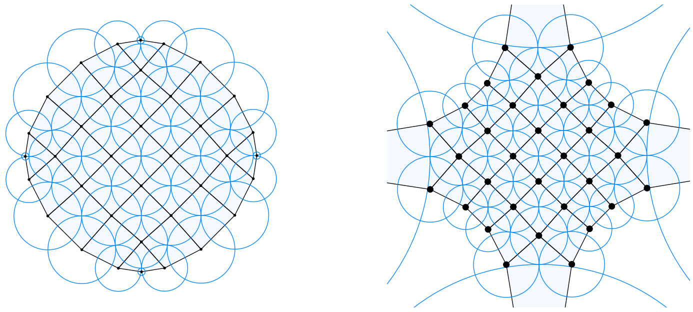

Figure 4. An orthogonal circle pattern and its dual. The boundary angles the dual pattern are $2\pi - \varphi_{ij}$ resp. $\pi - \varphi_{ij}$ depending on whether the degree of the boundary vertex is 3 or 2.

Note that the angles at interior vertices still sum up to 2π, but the angles at the boundary vertices change as shown in Fig. 4.

Now let us go back to the one parameter family $\mathcal{R}^\delta$ of ring patterns defined in Cor. 2.5. To avoid that the radii go to infinity as $\delta \to \pm\infty$ we scale the entire pattern by $2e^{-|\delta|}$. So the radii of the one parameter family of ring patterns are:

$$r^\delta_{m,n} = 2e^{-|\delta|}\sinh(\rho_{m,n} + \delta) \quad \text{and} \quad R^\delta_{m,n} = 2e^{-|\delta|}\cosh(\rho_{m,n} + \delta).$$

In the limit $\delta \to \pm\infty$ the areas of the rings tend to zero and for the radii we have:

$$\lim_{\delta\to\pm\infty} r^\delta_i = \lim_{\delta\to\pm\infty} 2e^{-|\delta|}\frac{1}{2}(e^{\rho_i+\delta} - e^{-\rho_i-\delta}) = e^{\pm\rho_i}\,,$$
$$\lim_{\delta\to\pm\infty} R^\delta_i = \lim_{\delta\to\pm\infty} 2e^{-|\delta|}\frac{1}{2}(e^{\rho_i+\delta} + e^{-\rho_i-\delta}) = e^{\pm\rho_i}.$$

Limit $\delta \to \infty$. For $\delta > -\min_{v_i\in G}\rho_i$ we have $\rho^\delta_i = \rho_i + \delta > 0$ for all $v_i \in G$. So considering the limit as $\delta \to \infty$ all ρ^δ_i will be positive and the angles of the circle pattern $\mathcal{C}$ (equation (3)) are exactly those of the ring pattern $\mathcal{R}^\delta$ given in Lemma 2.3. Furthermore, for $\delta \to \infty$, we obtain rings with area 0 since the outer and inner radii both converge to e^{ρ_i}. The neighboring circles intersect orthogonally because inner and outer circles of the orthogonal ring pattern are intersecting orthogonally in the entire one parameter family. The limit circles form a Schramm type orthogonal circle pattern.

Limit $\delta \to -\infty$. For $\delta < -\max_{v_i\in G}\rho_i$ all $\rho^\delta_i = \rho_i + \delta < 0$. By Lemma 2.3 the angles of the ring pattern for negative ρ_i are given by

$$\varphi_{ij} = -2\arctan(e^{\rho_i-\rho_j}) = -\pi + \arctan(e^{(-\rho_i)-(-\rho_j)})$$

and correspond to the angles of the dual pattern $\mathcal{C}^*$ with opposite orientation. As equation (2) is satisfied for all δ, we obtain the dual orthogonal circle pattern $\mathcal{C}^*$ (with opposite orientation) in the limit.

Corollary 3.1. *Let $\mathcal{R}^\delta$ be a one parameter family of orthogonal ring patterns with $\rho^\delta_i = \rho_i + \delta$ for $\rho_i \in \mathbb{R}$ as described in Cor. 2.5. Then for $\delta \to \infty$*

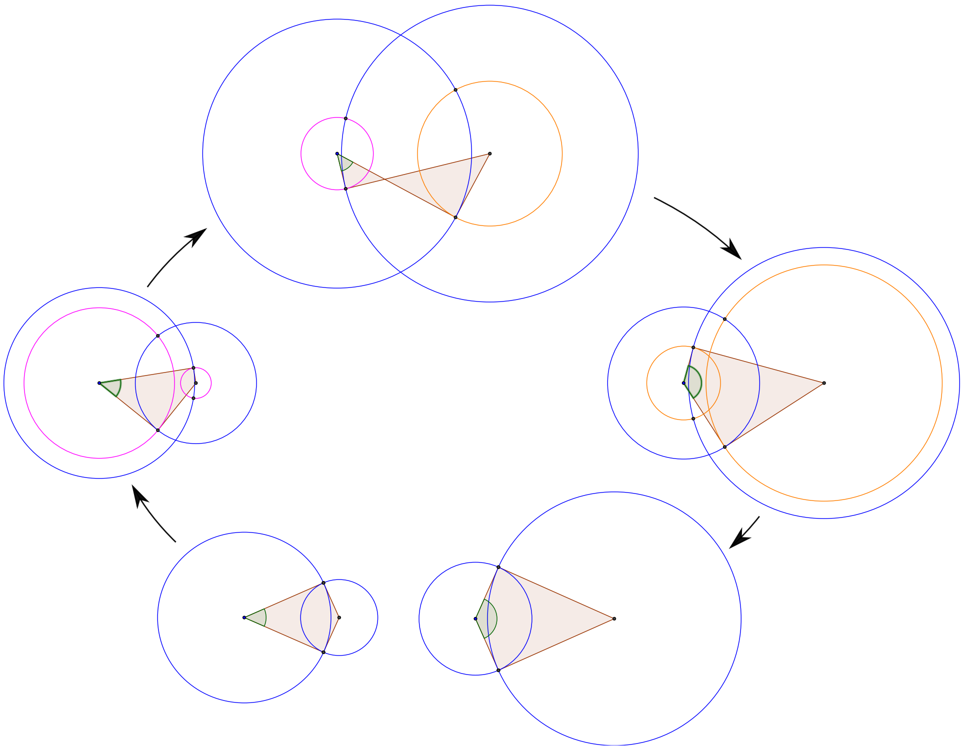

Figure 5. Deformation of a cyclic quadrilateral defined by two orthogonally intersecting rings. The bottom left and bottom right show the limits of the ring pattern as the area of the ring goes to zero. Positive radii are indicated by orange, negative radii (i.e., negative ρ) are indicated by pink circles. The angle associated with the left vertex is shown in green.

we obtain an orthogonal circle pattern $\mathcal{C}$ with logarithmic radii ρ_i and for $\delta \to -\infty$ we obtain the dual circle pattern $\mathcal{C}^*$ with logarithmic radii $-\rho_i$.

For a better understanding of the deformation, the one parameter family of cyclic quadrilaterals associated to a single edge (v_i, v_j) is shown in Fig. 5: Assume that ρ_i and ρ_j are both positive and $\rho_i < \rho_j$. Then the deformation starts with an embedded cyclic quadrilateral (center right). For $\delta \to \infty$ we obtain two orthogonally intersecting circles with radii e^{ρ_i} and e^{ρ_j} that form a kite (bottom right). When $\delta \searrow -\rho_i$ one of the edges at v_i shrinks to a point and reverses its direction as $\rho_i + \delta$ changes its sign from $+$ to $-$. If $-\rho_j < \delta < -\rho_i$ then $r_i^\delta < 0$ and we obtain a non-embedded quadrilateral (top center). Again as $\delta \searrow -\rho_j$ one edge at v_j shrinks to a point and changes its direction as $\rho_j + \delta$ changes sign (center left) and we obtain an embedded quadrilateral with negative orientation. For $\delta \to -\infty$ the areas of the rings go to zero and we obtain two orthogonally intersecting circles with radii $e^{-\rho_i}$ and $e^{-\rho_j}$ (bottom left). In the limit for $\rho \to \pm\infty$ we can consider the deformation of a point ($\rho = -\infty$) to a line ($\rho = \infty$).

4. Doyle spiral, Erf, and z^α ring patterns

In this section we will have a look at some known orthogonal circle patterns and consider their ring pattern analogs and deformations.

4.1. **Doyle spirals.** Doyle spirals for the square lattice have been constructed by Schramm [6]. For $x + iy \in \mathbb{C} \setminus \{0\}$ Schramm defines radii by $r_{m,n} = |e^{(x+iy)(m+in)}|$. Taking the logarithm we obtain the logarithmic radii $\rho_{m,n} = mx - ny$. We will take these radii as a definition of the Doyle spiral ring pattern.

Proposition 4.1 (Doyle spiral ring pattern)**.** *Let $x + iy \in \mathbb{C} \setminus \{0\}$ be a complex number. The* Doyle spiral ring pattern *is given by the ρ-radii $\rho_{m,n} = mx - ny$ for $(m, n) \in \mathbb{Z}^2$.*

By Lemma 2.3 the angles of the cyclic quadrilaterals at the edges are given by

$$\varphi_{(m,n),(m+1,n)} = \begin{cases} \pi - 2\arctan(e^{x}) & \text{if } \rho_{m,n} > 0 \\ -2\arctan(e^{x}) & \text{if } \rho_{m,n} < 0 \end{cases} \quad \text{and}$$

$$\varphi_{(m,n),(m,n+1)} = \begin{cases} \pi - 2\arctan(e^{-y}) & \text{if } \rho_{m,n} > 0 \\ -2\arctan(e^{-y}) & \text{if } \rho_{m,n} < 0 \end{cases}$$

Looking closer at the signs of the ρ-radii we observe that

$$\rho_{m,n} > 0 \Leftrightarrow mx > ny \qquad \text{and} \qquad \rho_{m,n} < 0 \Leftrightarrow mx < ny.$$

So the signs of the ρ-radii change across the line $\{(m, n) \in \mathbb{Z}^2 \,|\, mx = ny\}$ and hence does the orientation of the flowers. If we restrict to the parts $\{(m, n) \in \mathbb{Z}^2 \,|\, mx > ny\}$ (resp. $\{(m, n) \in \mathbb{Z}^2 \,|\, mx < ny\}$) we see that the angles are constant for all horizontal edges $(m, n)(m + 1, n)$ and all vertical edges $(m, n)(m, n + 1)$. Thus we can define a Doyle spiral ring pattern by two angles α and β, one for the horizontal and one for the vertical direction. This is the characteristic property for the Doyle spiral circle pattern.

Consider the one parameter family $\mathcal{R}^{\delta}$ of orthogonal ring patterns as described by Cor. 2.5. The angles along the horizontal and vertices edges stay constant in the two halfspaces. As in the general case discussed in the previous section, all ρ's become positive for $\delta \to \infty$ (resp. negative for $\delta \to -\infty$) and we obtain a Doyle spiral and its dual as constructed by Schramm (see Fig. 6).

4.2. **Erf pattern.** For analogs to Schramm's $\sqrt{i}$-Erf pattern let us have a look at the corresponding radius function given in [6] $r_{m,n} = e^{amn}$ for $(m, n) \in \mathbb{Z}^2$ and $a \in \mathbb{R}$, $a > 0$. Taking the logarithm we obtain $\rho_{m,n} = amn$. As in case of the Doyle spiral we will use this function to define the corresponding ring patterns.

Proposition 4.2 (Erf ring pattern)**.** *Let $a \in \mathbb{R}, a > 0$. The* Erf ring pattern *is given by the ρ-radii $\rho_{m,n} = amn$ for $(m, n) \in \mathbb{Z}^2$.*

The angles in the pattern are given by

$$\varphi_{(m,n),(m+1,n)} = \begin{cases} \pi - 2\arctan(e^{-an}) & \text{if } \rho_{m,n} > 0 \\ -2\arctan(e^{-an}) & \text{if } \rho_{m,n} < 0 \end{cases} \quad \text{and}$$

$$\varphi_{(m,n),(m,n+1)} = \begin{cases} \pi - 2\arctan(e^{-am}) & \text{if } \rho_{m,n} > 0 \\ -2\arctan(e^{-am}) & \text{if } \rho_{m,n} < 0 \end{cases}$$

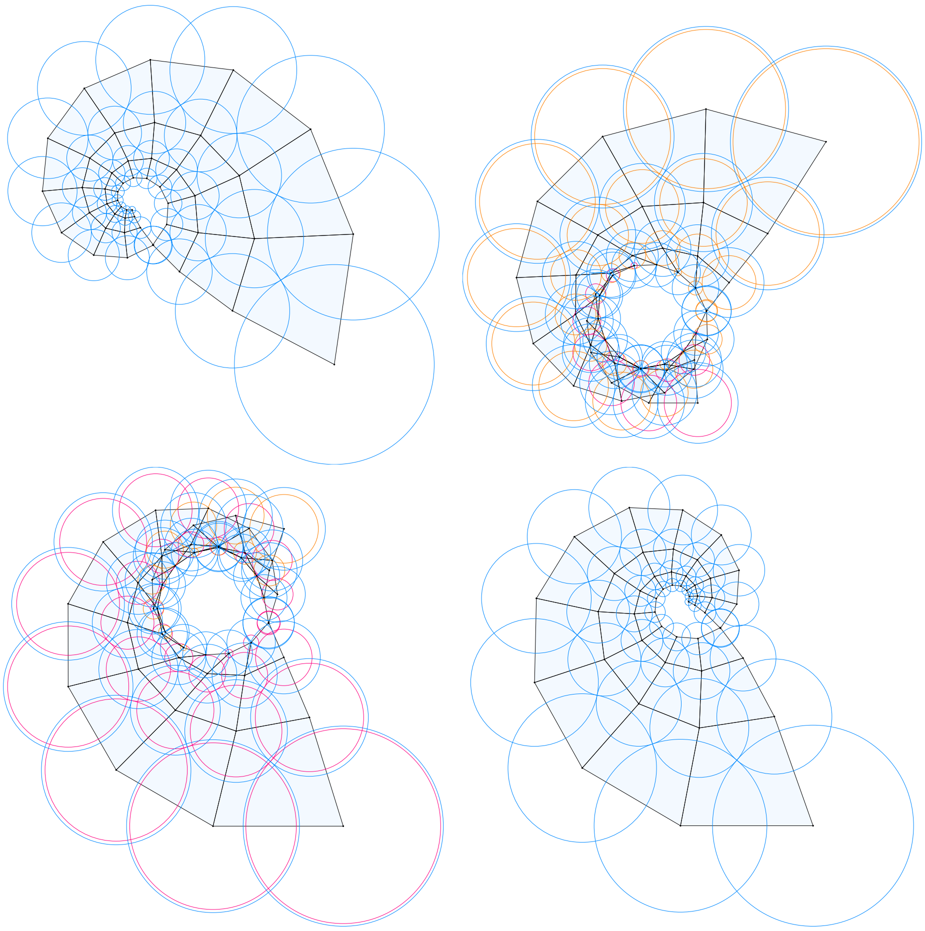

Figure 6. Deformation of an orthogonal circle pattern (top left) into its dual (bottom right) through a one parameter family of ring patterns (top right and bottom left). We see how the orientation of the quadrilaterals flips during the deformation. The innermost vertex in the top left circle patterns becomes the outermost vertex in the bottom right circle pattern.

As $\rho_{m,n} = amn$ the ρ-radii change signs at the coordinate axes. In the four orthants, the angles along the horizontal and the vertical parameter lines are constant.

If we consider the one parameter family of ring patterns defined in Cor. 2.5 we see that in the limit $\delta \to \infty$ we obtain the $\sqrt{i}$-SG Erf circle patterns constructed by Schramm. For $\delta \to -\infty$ we obtain a pattern with $\rho^*_{m,n} = -amn$. This is the same pattern as for a since $\rho^*_{m,n} = \rho_{-m,n}$.

4.3. z^α **and logarithm patterns.** In [2] the authors defined an orthogonal circle pattern $\mathcal{C}(z^\alpha)$ as a discretization of the complex map $z \mapsto z^\alpha$ for $\alpha \in (0, 2)$. The radius function of the circle pattern is given by the following identities (cf. [2, Thm. 3, equation (10, 11)]) on a subset of $\mathbb{Z}^2$ given by

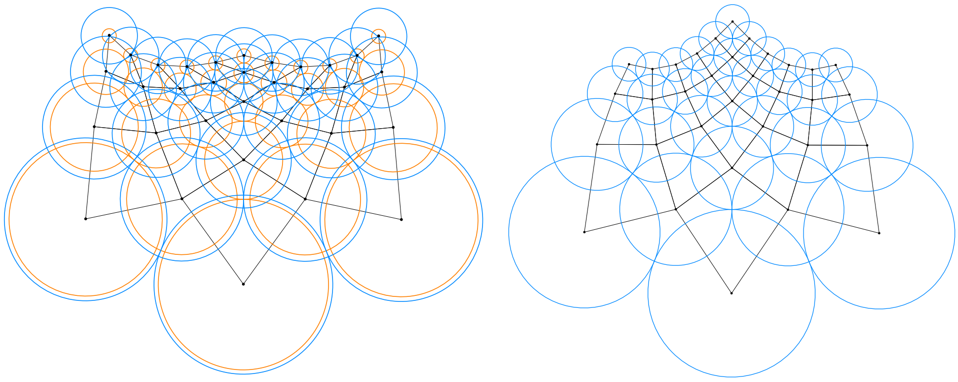

Figure 7. An Erf ring pattern (left) and the corresponding limit circle pattern.

$V = \{(m,n) \,|\, m \geq |n|\}$:

$$r_{m,n}r_{m+1,n}(-2n-\alpha) + r_{m+1,n}r_{m+1,n+1}(2(m+1)-\alpha) \\ + r_{m+1,n+1}r_{m,n+1}(2(n+1)-\alpha) + r_{m,n+1}r_{m,n}(-2m-\alpha) = 0$$

for $V \cup \{(-m, m-1) \,|\, m \in \mathbb{N}\}$ and

$$(m+n)(r_{m,n}^2 - r_{m+1,n}r_{m,n-1})(r_{m,n+1} + r_{m+1,n}) \\ + (n-m)(r_{m,n}^2 - r_{m,n+1}r_{m+1,n})(r_{m+1,n} + r_{m,n-1}) = 0$$

for interior vertices $V \setminus \{(\pm m, m) \,|\, m \in \mathbb{N}\}$ with initial condition $r_{0,0} = 1$ and $r_{0,1} = \tan \frac{\alpha\pi}{4}$.

It is known that the dual pattern of z^α is given by $z^{2-\alpha}$, e.g., the dual circle pattern of $\mathcal{C}(z^{2/3})$ is $\mathcal{C}(z^{4/3}) = (\mathcal{C}(z^{2/3}))^*$ shown in Fig. 8 (top left and bottom right). Based on the logarithmic radii of these patterns we construct a one parameter family of ring patterns that interpolates between the two patterns.

An orthogonal circle pattern for z^2 can be defined by considering a special limit for $\alpha \to 2$. The radii of the z^2 pattern are defined in [2, Sect. 5]. The dual of z^2 is the logarithm map $\log z$. In each of the corresponding orthogonal circle patterns, one of the circles degenerates. In case of z^2 one of the circles has radius 0, i.e., the circle degenerates to a point and the logarithmic radius is negative infinity. Consequently, one of the circles in the $\log z$ pattern has radius infinity, i.e., the circle degenerates to a line and the logarithmic radius is positive infinity. We illustrate the one parameter deformation of z^2 to $\log(z)$ in Fig. 9.

5. Variational description

The construction of a ring pattern is very similar to the construction of an orthogonal circle pattern since the equations at the interior vertices are the same (see Thm. 2.4). For (not necessarily orthogonal) circle patterns there exists a convex variational principle [5] in terms of the logarithmic radii. In this section we will consider subcomplex G of $\mathbb{Z}^2$ whose boundary consists of zigzag edges only as shown in Fig. 10. For planar orthogonal circle patterns

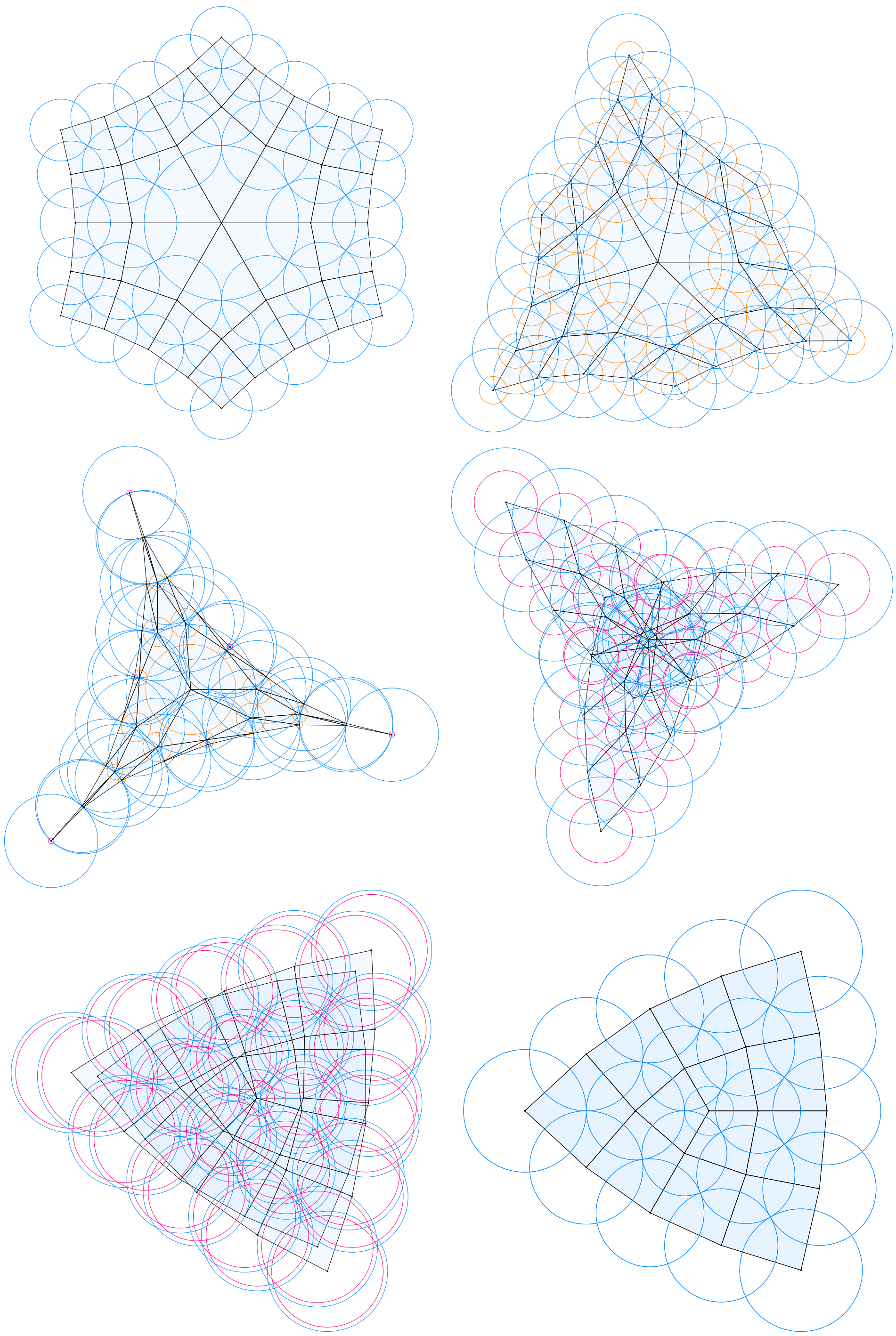

Figure 8. One parameter family of orthogonal ring patterns interpolating between the orthogonal circle pattern for $z \mapsto z^{2/3}$ (top left) and the dual pattern for $z^{4/3}$ (bottom right)

the functional is given by:

$$S_{Euc}(\rho) = \sum_{v_i \bullet\!\bullet v_j} \Big(\operatorname{Im} \operatorname{Li}_2(ie^{\rho_j - \rho_i}) + \operatorname{Im} \operatorname{Li}_2(ie^{\rho_i - \rho_j}) - \frac{\pi}{2}(\rho_i + \rho_j) \Big) + \Phi_i \sum_{v_i} \rho_i \,,$$

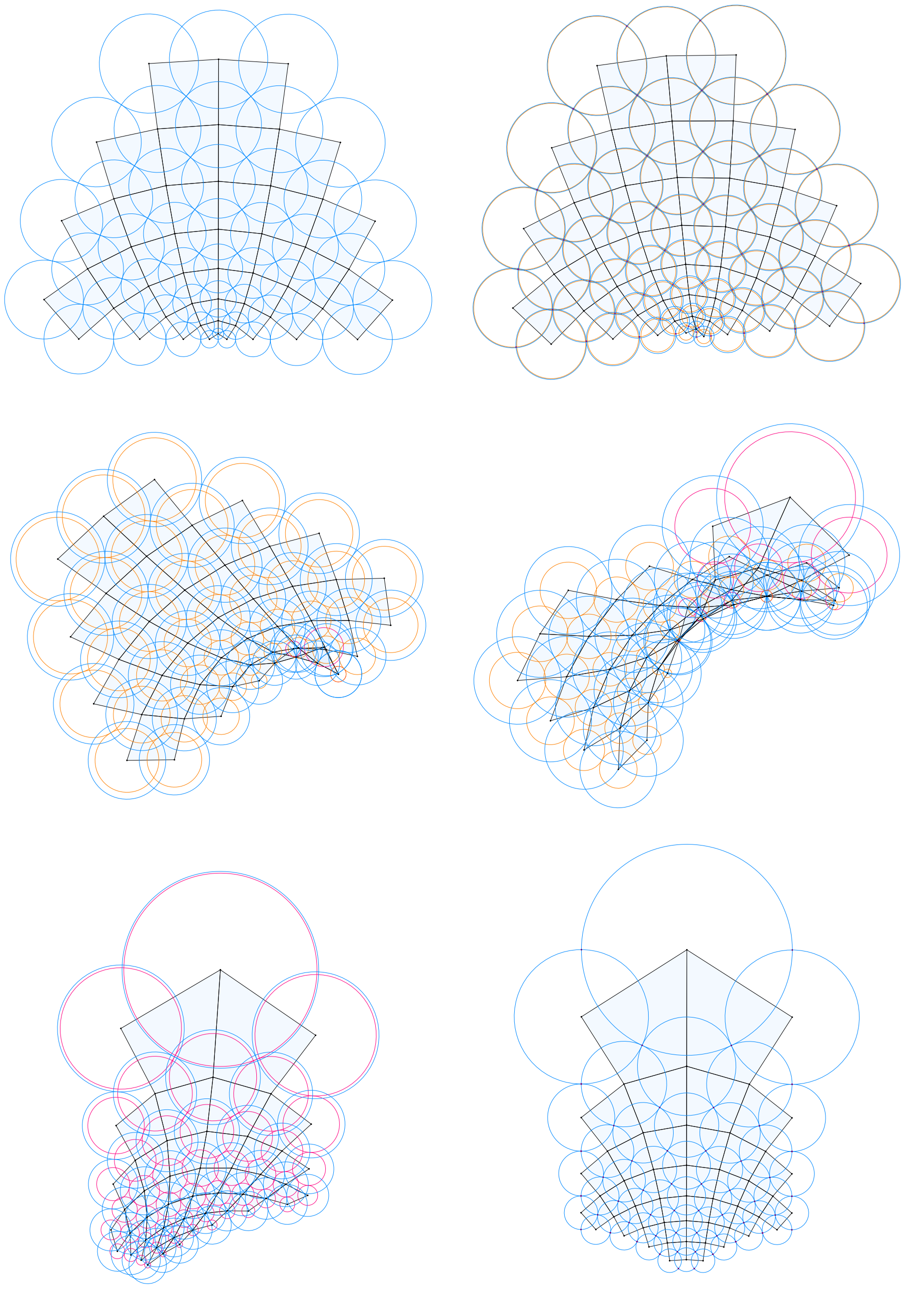

Figure 9. Orthogonal ring patterns interpolating between the circle patterns for z^2 and its dual pattern for $\log z$.

where $\Phi_i = 2\pi$ for interior vertices and $\Phi_i \in (0, 2\pi)$ for boundary vertices and Li_2 is the dilogarithm function. The first sum is taken over all edges and the second sum over all vertices of G. For a flat euclidean orthogonal circle pattern we need to require that boundary angles sum up to $(n-2)\pi$ where n is the number of boundary vertices. The critical points of the functional satisfy the condition that all the kite angles around the vertices v_i sum up to Φ_i. So for the interior vertices with $\Phi_i = 2\pi$ we obtain exactly equation (2)

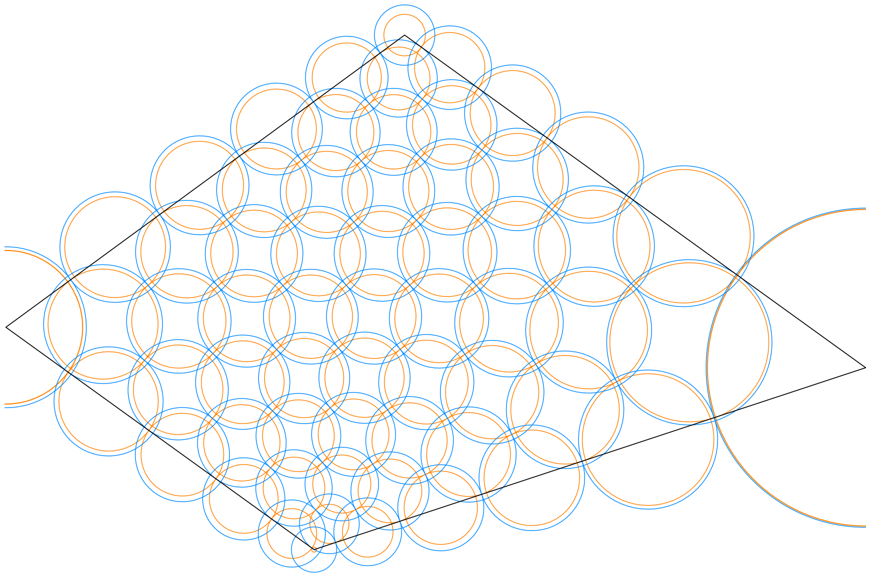

Figure 10. An orthogonal ring pattern computed using the variational principle with Neumann boundary conditions. The prescribed angles are π for the boundary vertices of degree 2 and 2π for the vertices of degree 4. The shape is governed by the four angles prescribed for the four boundary vertices of degree 3.

and for the boundary edges the prescribed curvature. As the functional is convex [5, Prop. 1,2] there exists a unique Euclidean ring pattern with the prescribed boundary conditions.

To determine a solution we can either prescribe *Dirichlet boundary conditions* by prescribing the ρ's for the boundary rings or *Neumann boundary conditions* by specifying the curvatures Φ_i for the boundary vertices (see Fig. 10).

Acknowledgements. We thank Boris Springborn for fruitful discussions on circle patterns and variational principles and Nina Smeenk for the support in developing the software for creating the figures. This research was supported by the DFG Collaborative Research Center TRR 109 "Discretization in Geometry and Dynamics".

References

[1] V. E. Adler, A. I. Bobenko, and Y. B. Suris. Classification of integrable equations on quad-graphs. The consistency approach. *Comm. Math. Phys.*, 233(3):513–543, 2003.

[2] S. I. Agafonov and A. I. Bobenko. Discrete Z^γ and Painlevé equations. *International Mathematics Research Notices*, 2000(4):165–193, 01 2000.

[3] A. I. Bobenko and T. Hoffmann. S–conical cmc surfaces. Towards a unified theory of discrete surfaces with constant mean curvature. In A. I. Bobenko, editor, *Advances in Discrete Differential Geometry*. Springer, 2016.

[4] A. I. Bobenko, U. Pinkall, and B. A. Springborn. Discrete conformal maps and ideal hyperbolic polyhedra. *Geom. Topol.*, 19(4):2155–2215, 2015.

[5] A. I. Bobenko and B. A. Springborn. Variational principles for circle patterns and Koebe's theorem. *Trans. Amer. Math. Soc.*, 356(2):659–689, 2004.

[6] O. Schramm. Circle patterns with the combinatorics of the square grid. *Duke Math. J.*, 86(2):347–389, 1997.

[7] X. Tellier, L. Hauswirth, C. Douthe, and O. Baverel. Discrete CMC surfaces for doubly-curved building envelopes. In L. Hesselgren, A. Kilian, S. M. andKarl Gunnar Olsson, and O. S.-H. C. Williams, editors, *Advances in Architectural Geometry*, 2018.

Alexander I. Bobenko, Thilo Rörig

Institute of Mathematics, Secr. MA 8-4, TU Berlin, 10623 Berlin, Germany

Email: {bobenko,roerig}@math.tu-berlin.de

Tim Hoffmann

Dept. of Mathematics, TU Munich, 85748 Garching, Germany

Email: tim.hoffmann@ma.tum.de